



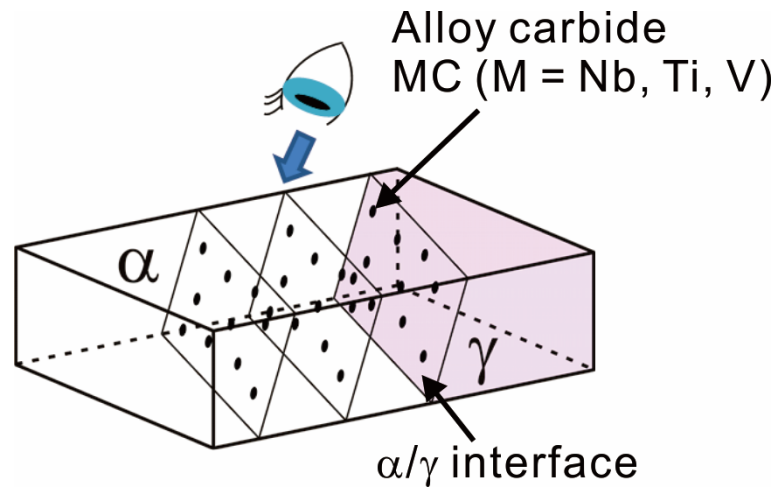
2018.7.5 17th ALEMI Meeting @ Citadelle Hotel, Metz, France

Nucleation of Vanadium Carbide Interphase Precipitation with Different Ferrite Growth Rate in Low Carbon Steels

Y.-J. Zhang, G. Miyamoto, T. Furuhashi

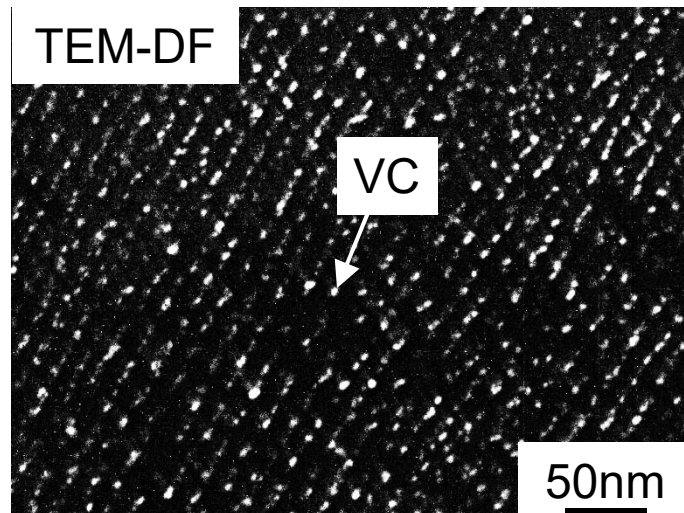
Institute for Materials Research, Tohoku University, Japan



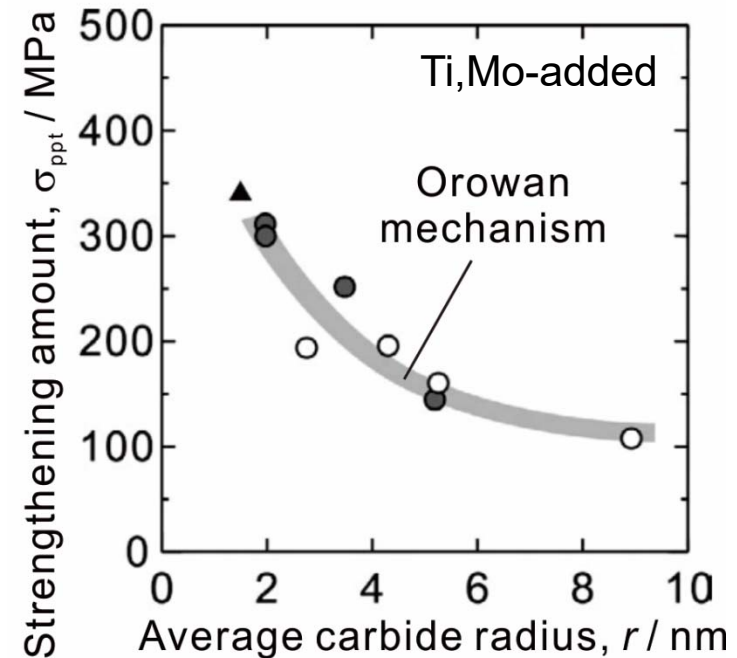


Periodic nucleation at migrating interface

V-added low carbon steel

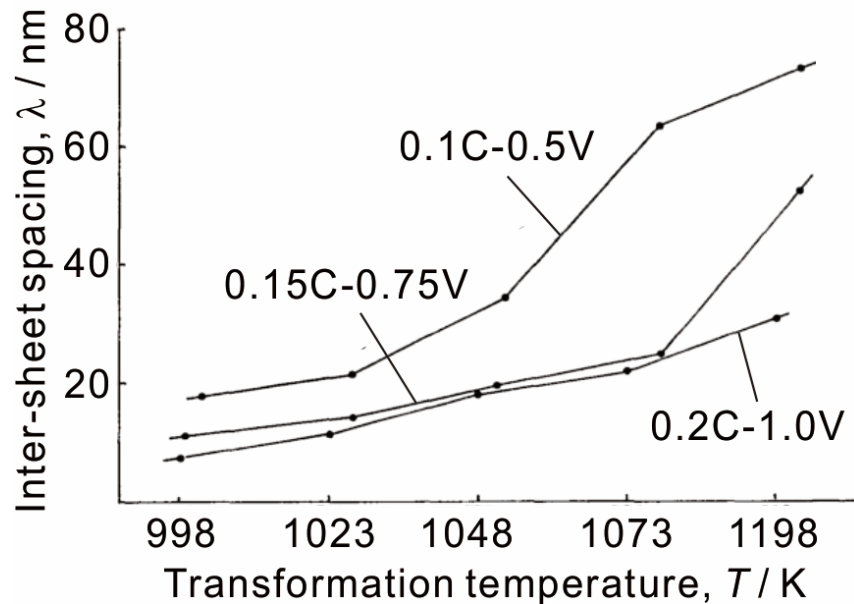


Precipitation strengthening

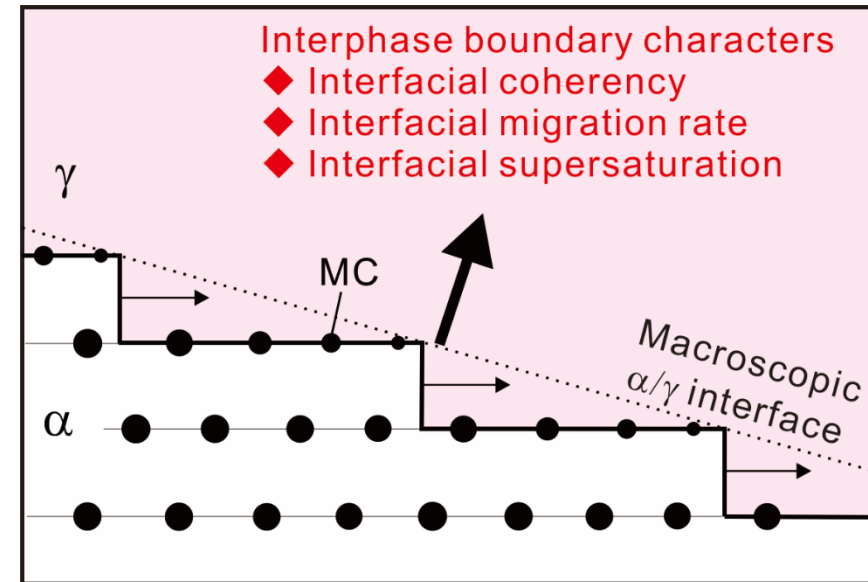


N. Kamikawa et al., *ISIJ Int.* 54 (2014) 212.

- Larger precipitation strengthening can be obtained by refining MC until nano size.



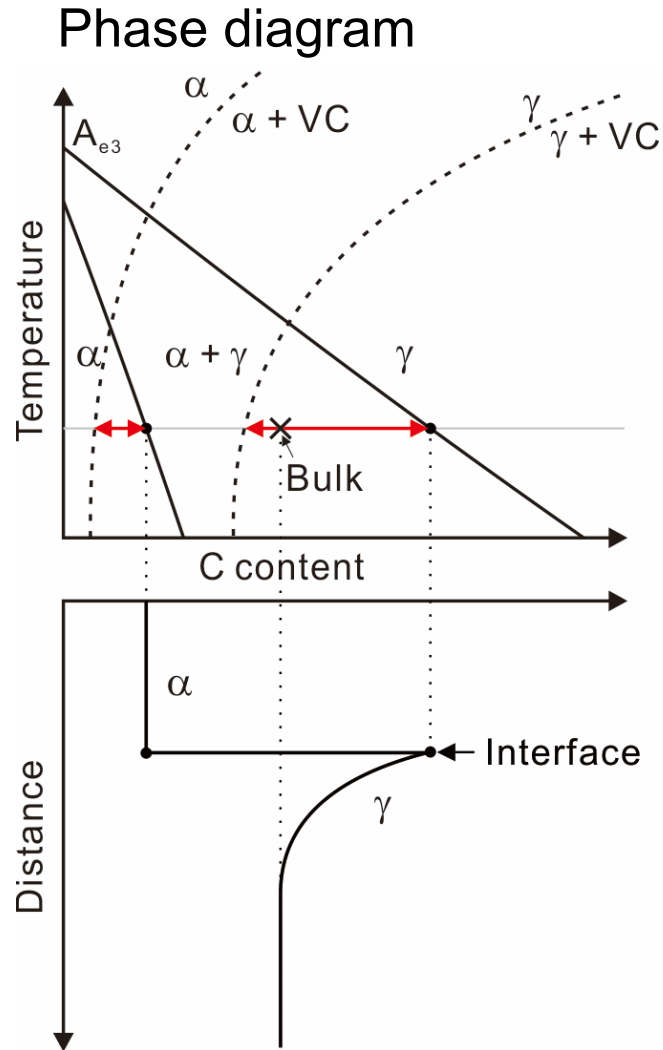
A.D. Batte et al., *Met. Sci. J.*, 7 (1973) 160.



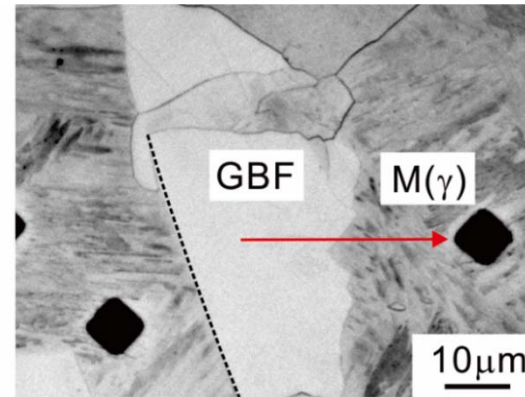
- | | | | |
|-------------------------------|---|--------------------|------------------|
| ● Interfacial coherency | → | Density of defects | } for nucleation |
| ● Interfacial migration rate | → | Time | |
| ● Interfacial supersaturation | → | Driving force | |



Variations in dispersion of interphase precipitation

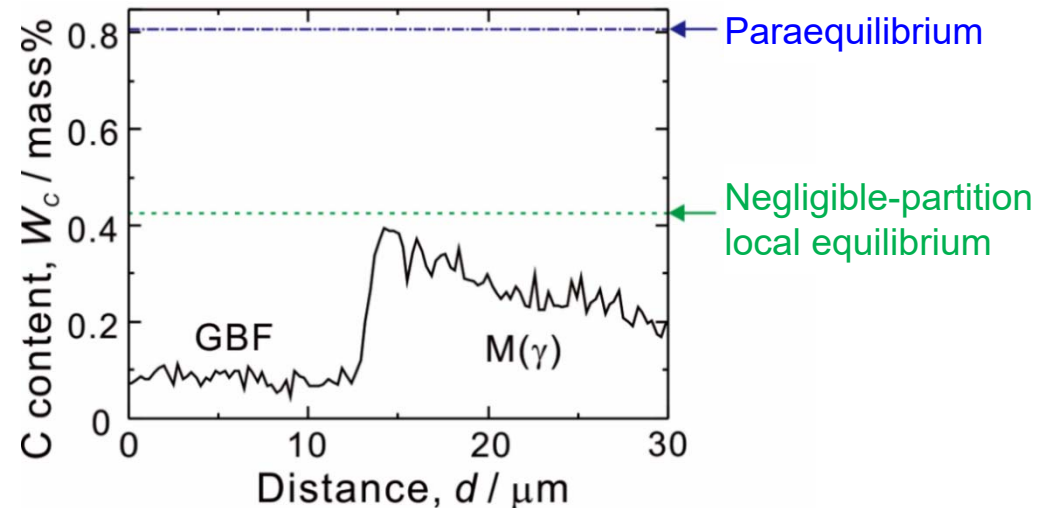


0.2C-0.4V, 963K, 0.3ks



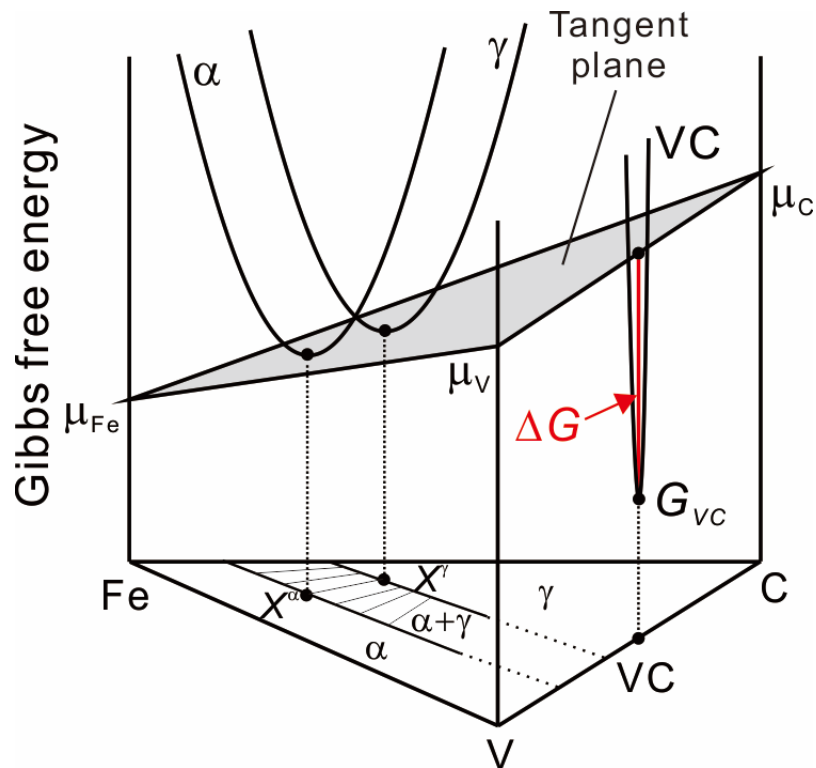
GBF: grain boundary α ;
M(γ): martensite

By electron probe microanalysis (EPMA)



Y.-J. Zhang et al., *Acta Mater.* 128 (2017) 166.

- Compared with PE model, NPLE model gives better prediction of α/γ phase equilibria in V-added low carbon steels.



By assuming 50at% V and 50at% C:

$$\Delta G = 0.5\mu_V + 0.5\mu_C - G_{VC}$$

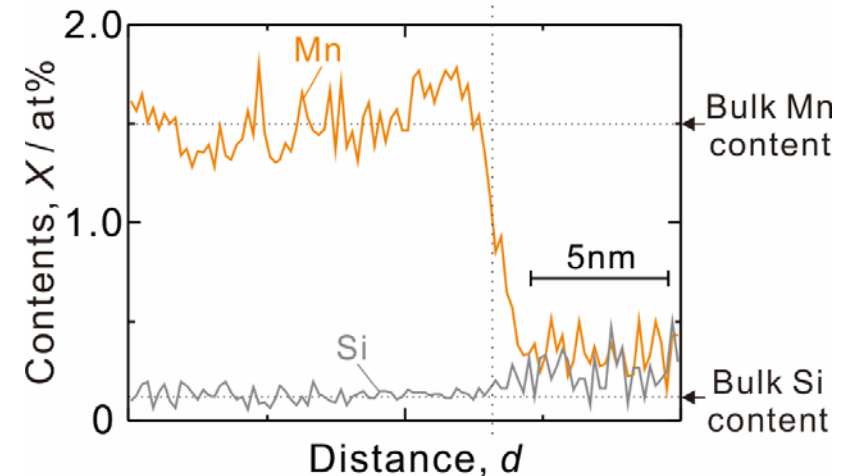
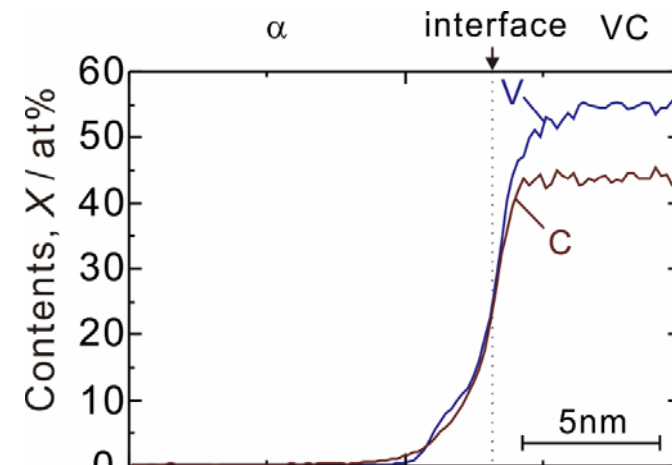
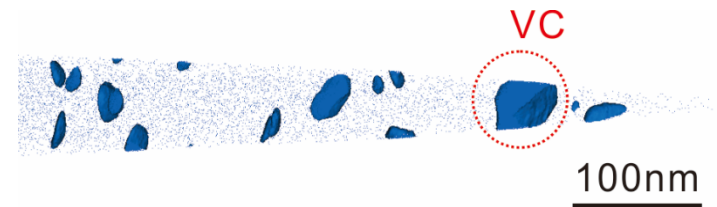
ΔG : driving force;

μ_i : chemical potential of i ;

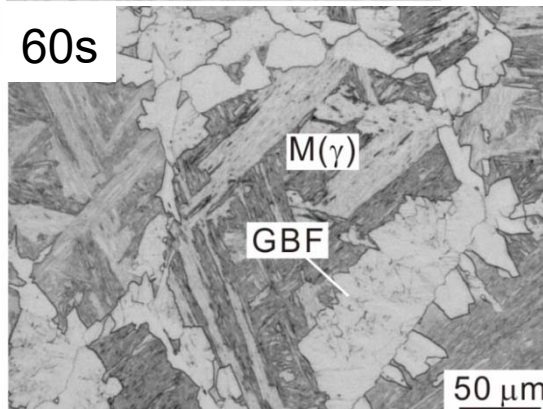
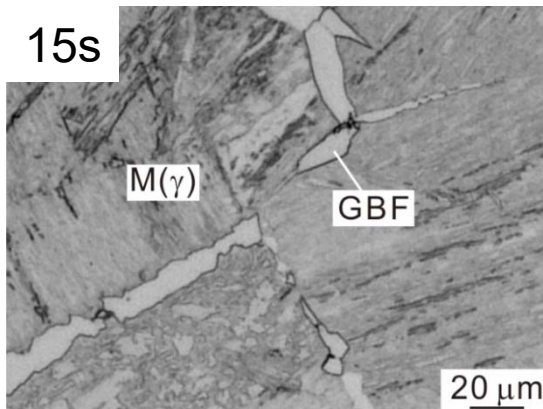
G_{VC} : free energy

(Segregation is neglected for simplicity)

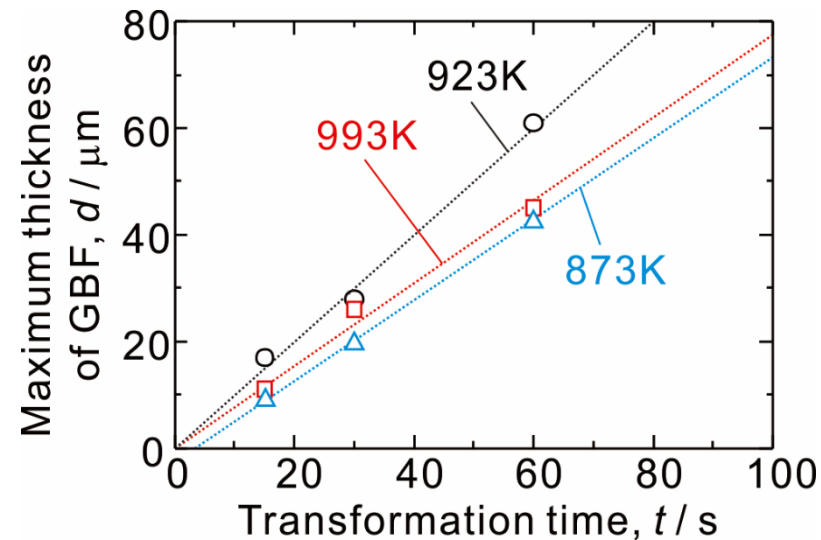
0.1C-0.4V, 923K, 172.8ks



0.1C-0.4V, 923K



GBF: grain boundary α ; M(γ): martensite



- α growth rate can be approximately estimated from maximum thickness of GBF.

Objective

Through quantitative analysis on dispersion of VC interphase precipitation formed under different conditions, we aimed to clarify the effects of α growth rate and driving force on interphase precipitation.

- Alloys (mass%)

0.1C-0.1V: Fe-0.1C-1.5Mn-0.05Si-**0.1V**

0.1C-0.2V: Fe-0.1C-1.5Mn-0.05Si-**0.2V**

0.1C-0.4V: Fe-0.1C-1.5Mn-0.05Si-**0.4V (Base)**

0.1C-0.4V: Fe-0.1C-**0.7Mn**-0.05Si-0.4V (**Low Mn**)

0.1C-0.4V: Fe-0.1C-1.3Mn-**0.4Si**-0.4V (**High Si**)

0.2C-0.4V: Fe-**0.2C**-1.5Mn-0.05Si-0.4V

0.2C-0.9V: Fe-**0.2C**-1.5Mn-0.05Si-**0.9V**

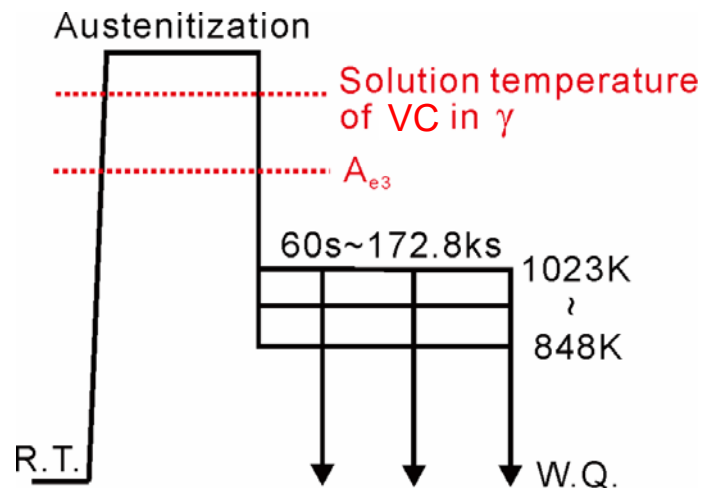
0.3C-1.3V: Fe-**0.3C**-1.5Mn-0.05Si-**1.3V**

Effect of driving force

Effect of α growth rate

Effect of driving force

- Heat treatment



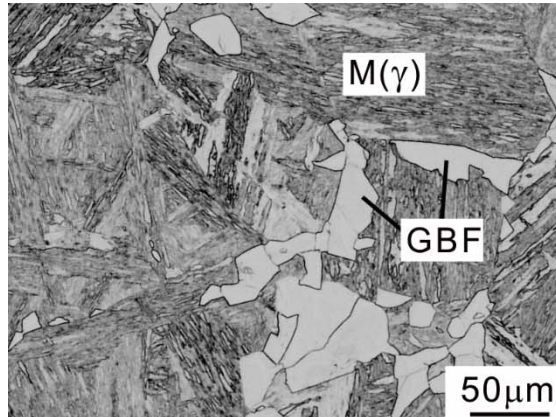
- Microstructural characterization

- Optical microscopy (OM)
- Scanning electron microscopy (SEM) / Electron backscatter diffraction (EBSD)
- Three-dimensional atom probe (3DAP)

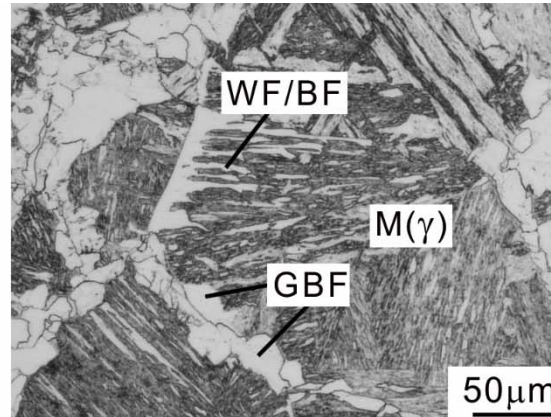
0.1C-0.4V (Base)

WF / BF: Widmanstatten / baintic α

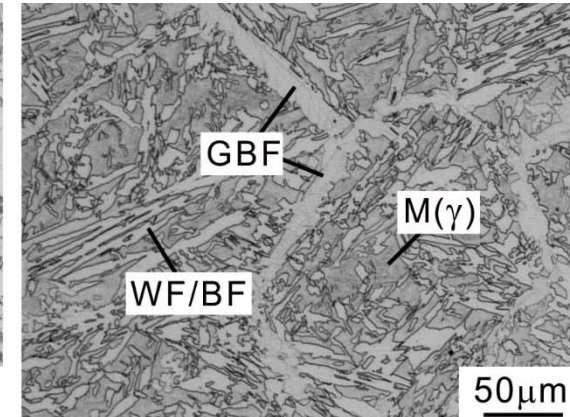
993K, 60s



923K, 60s



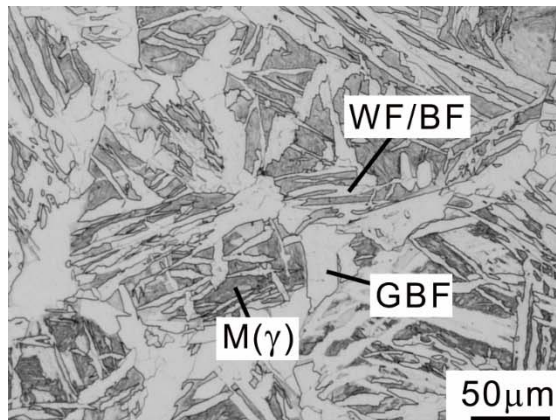
873K, 60s



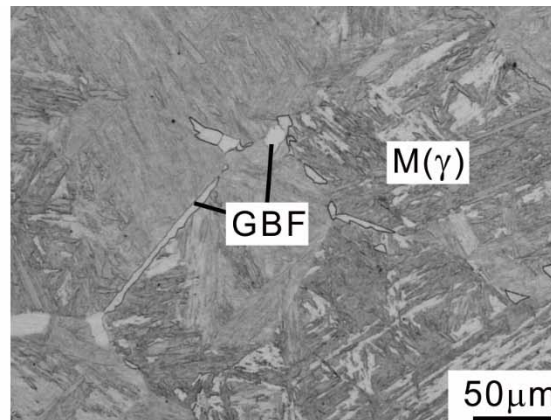
- α morphology changes from GBF into WF/BF by lowering temperature.

923K, 60s

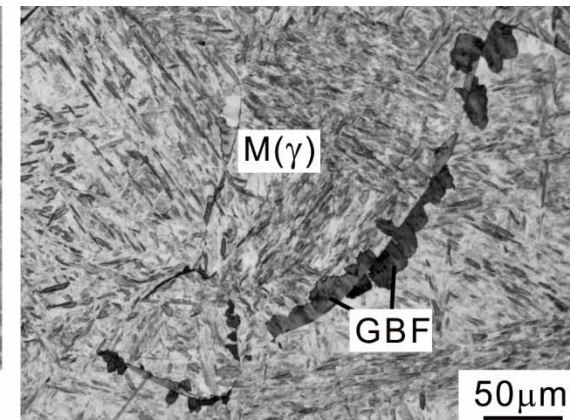
0.1C-0.1V



0.2C-0.4V



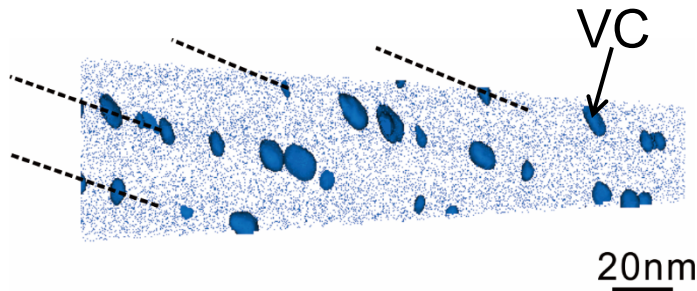
0.3C-1.3V



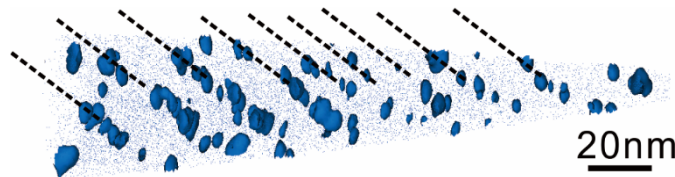
- Formation of WF/BF is suppressed by increasing V and C contents.

0.1C-0.4V (Base)

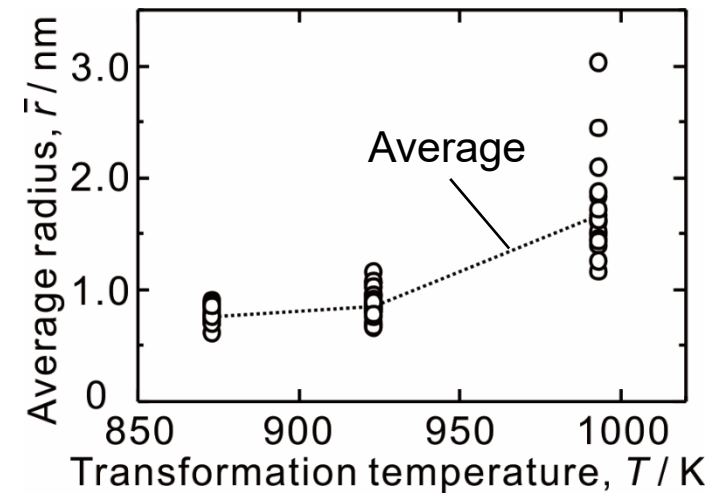
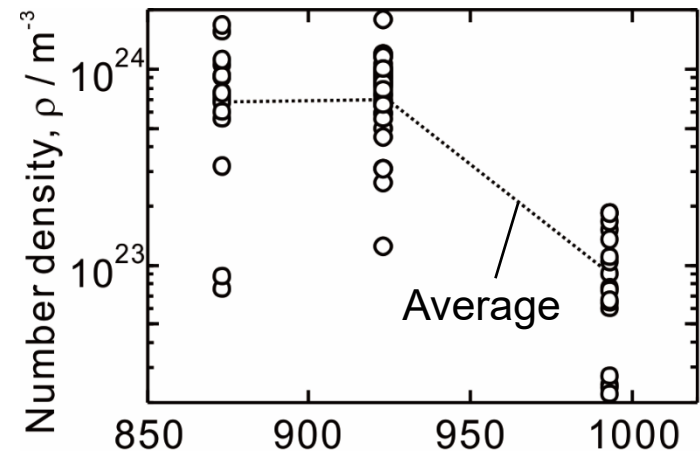
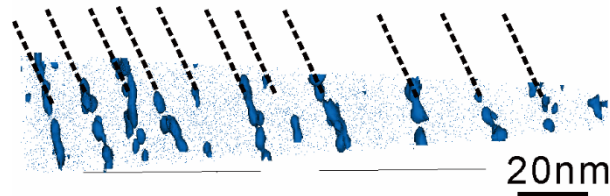
993K, 60s



923K, 60s



873K, 60s

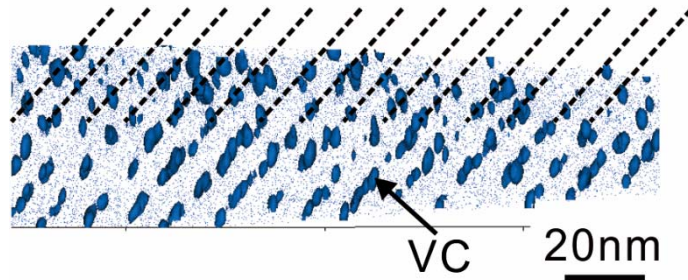


Y.-J. Zhang et al., *Acta Mater.* 84 (2015) 375.

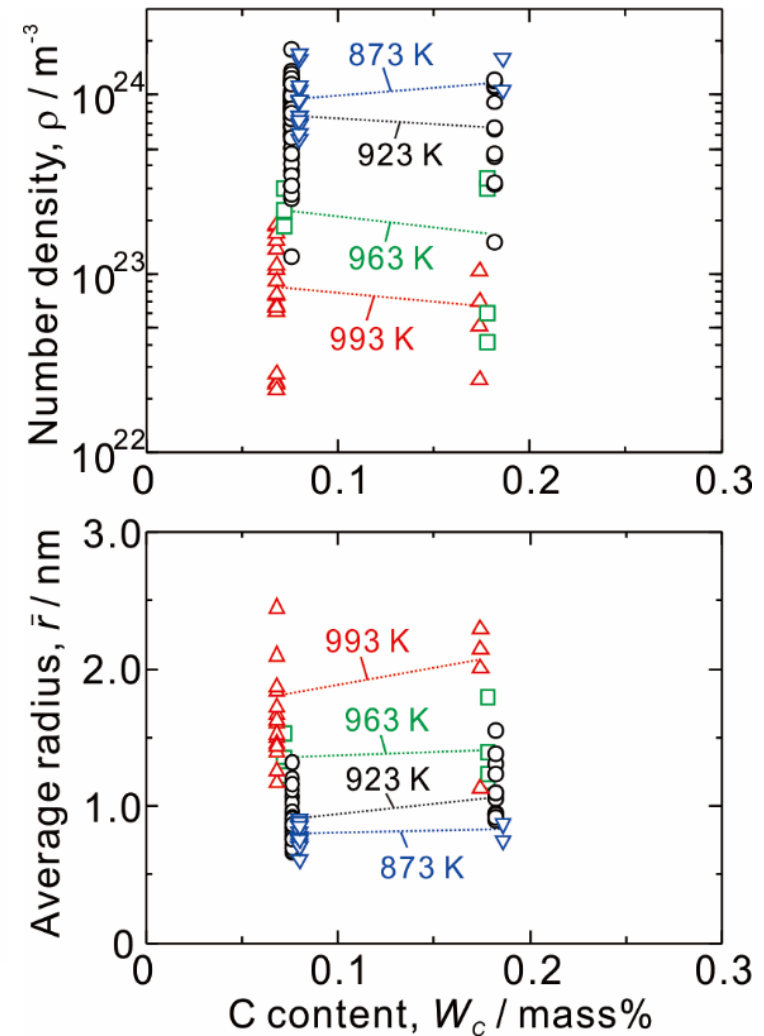
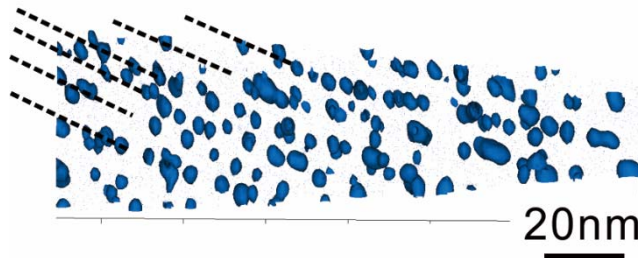
- Dispersion of VC becomes higher in number density and smaller in size by lowering transformation temperature.

923K, 60s

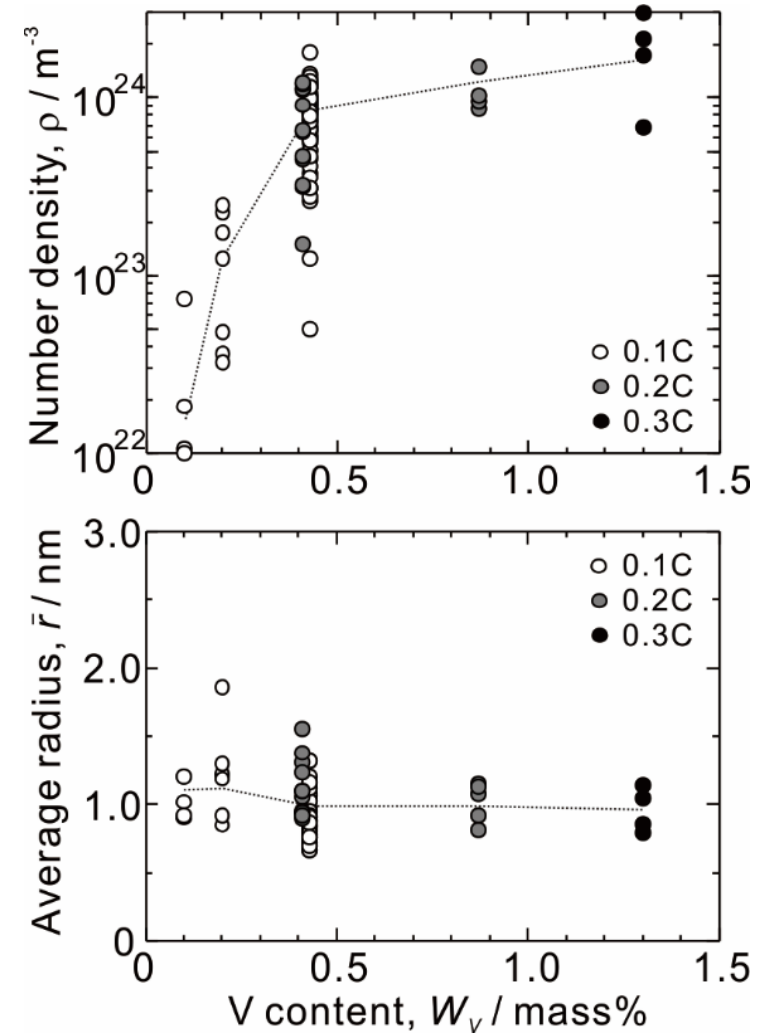
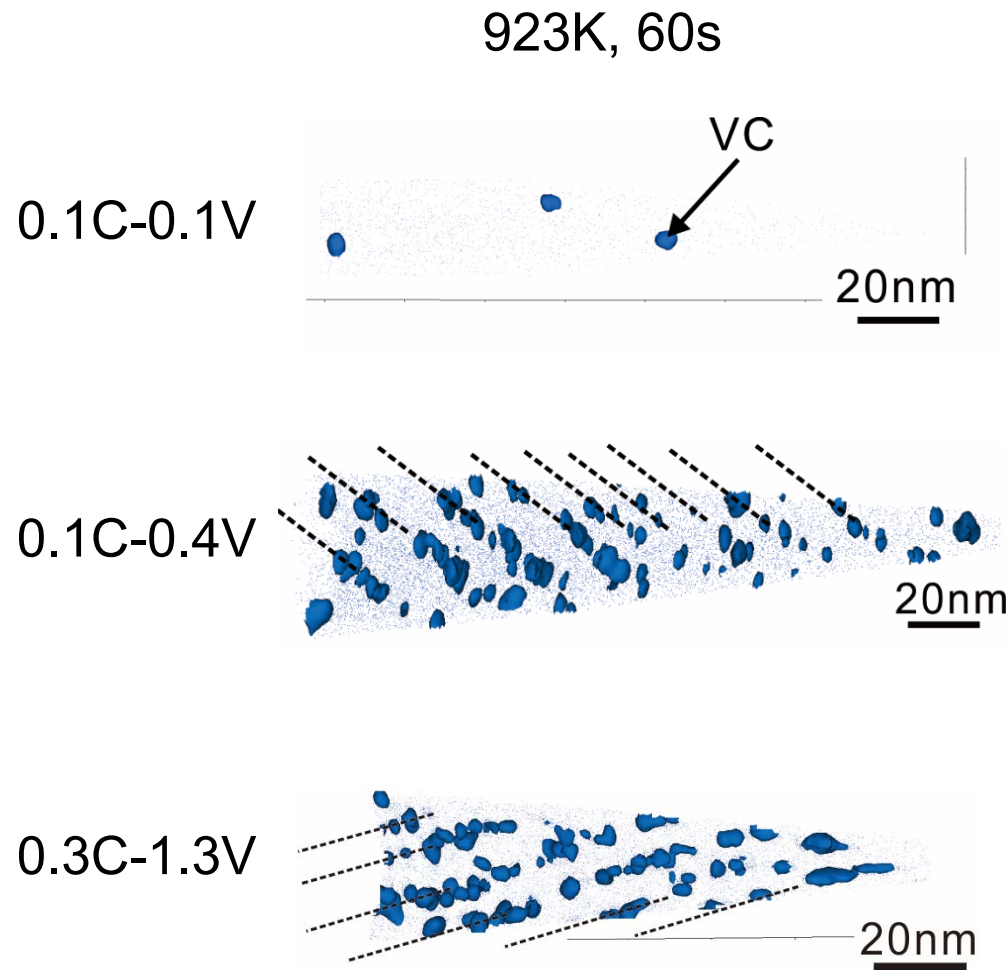
0.1C-0.4V



0.2C-0.4V



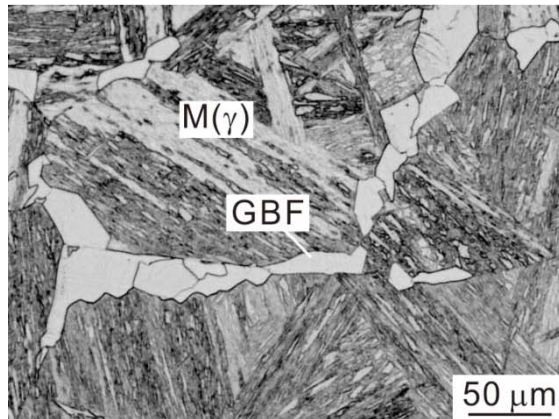
- Dispersion of VC is only slightly influenced by increasing bulk C content.



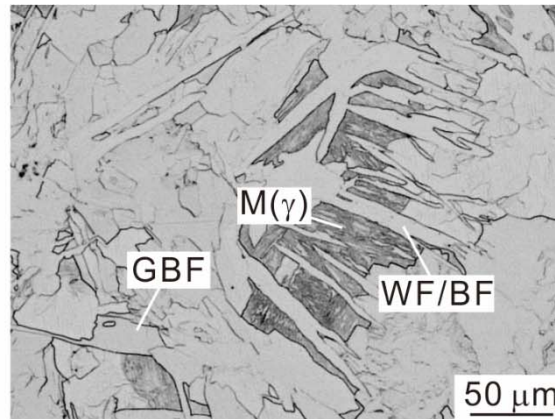
- Number density of VC is increased, while size of VC is slightly decreased by increasing V content.

993K, 60s

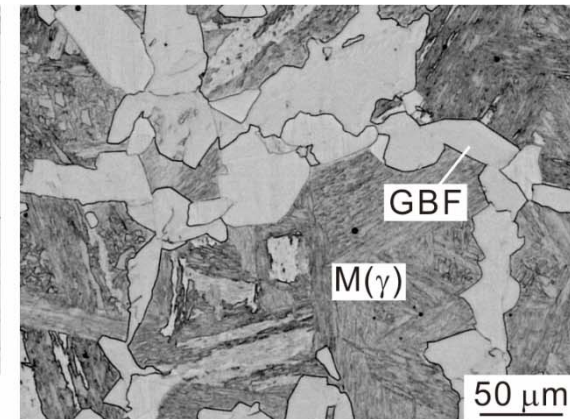
0.1C-0.4V (Base)



0.1C-0.4V (Low Mn)



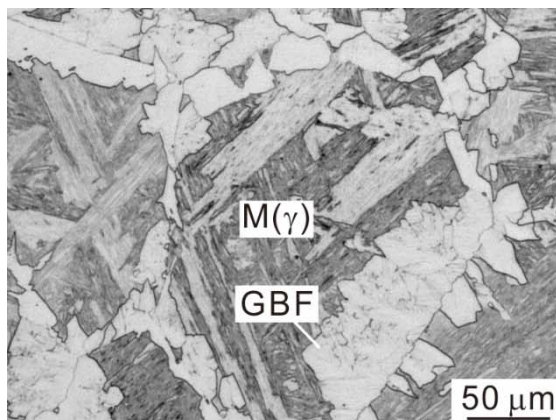
0.1C-0.4V (High Si)



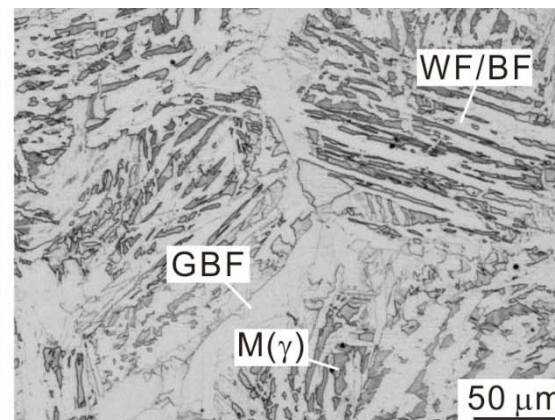
- α growth is greatly accelerated by reducing Mn or increasing Si content.

923K, 60s

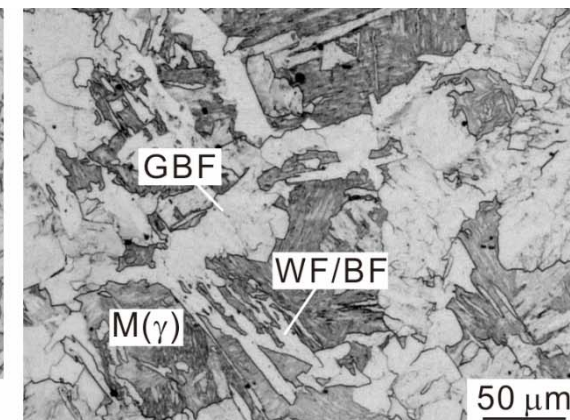
0.1C-0.4V (Base)



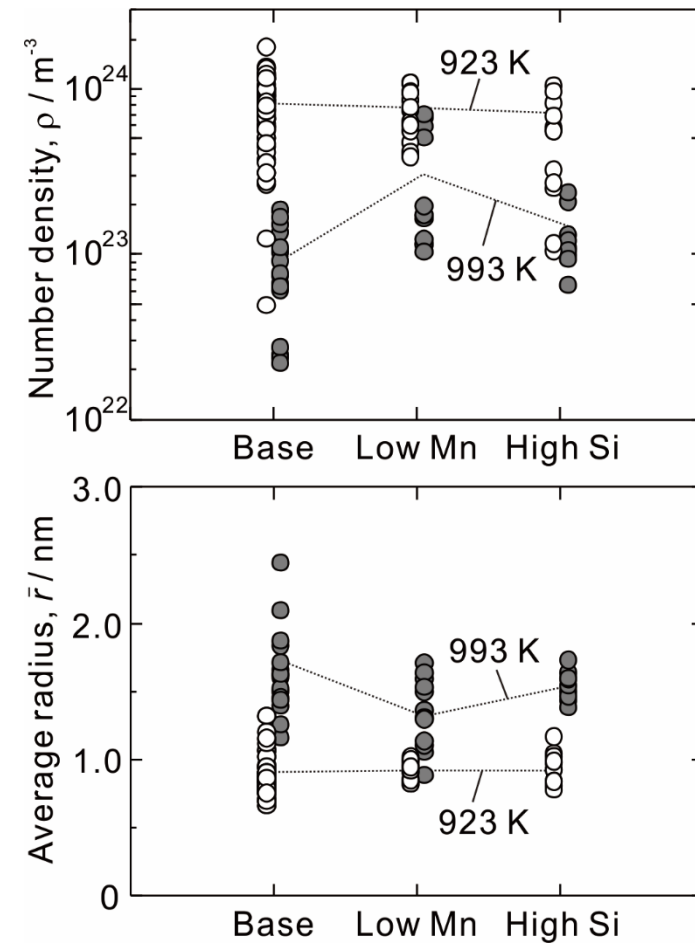
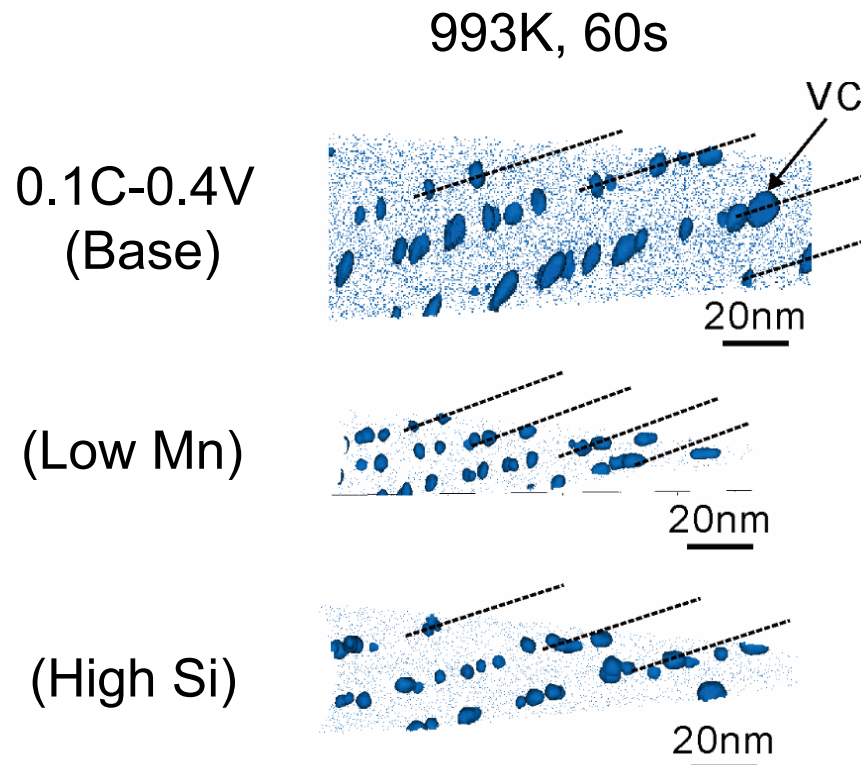
0.1C-0.4V (Low Mn)



0.1C-0.4V (High Si)

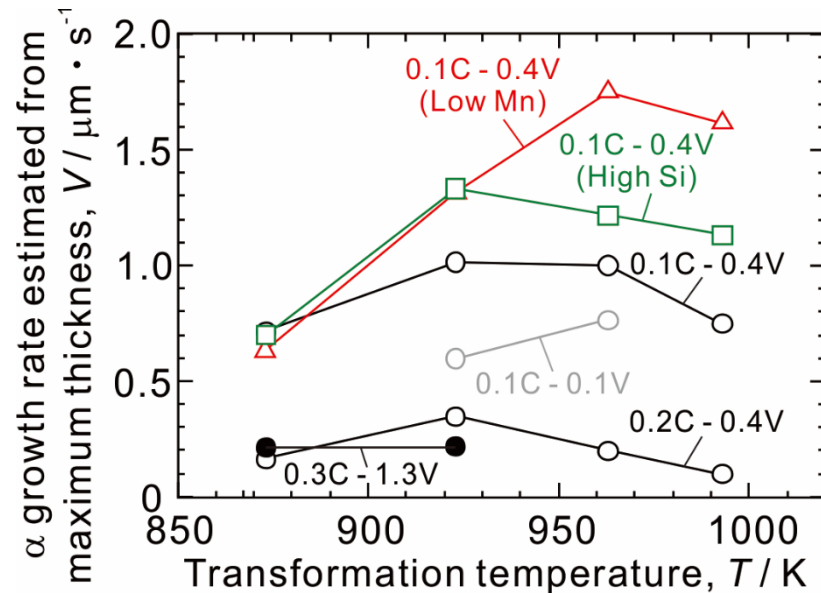


- WF/BF formation is promoted by reducing Mn or increasing Si content.



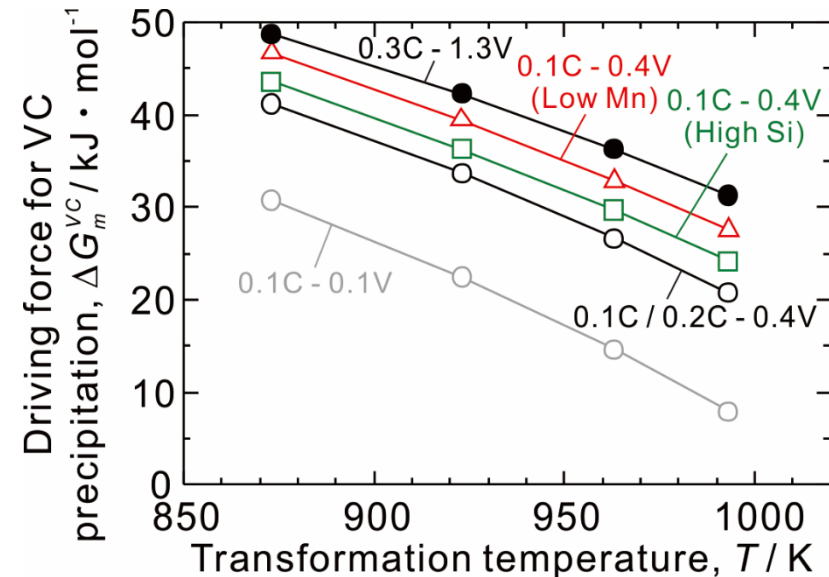
- Dispersion of VC is refined by reducing Mn or increasing Si content at higher temperature, but almost unchanged at lower temperature.

From maximum α thickness:

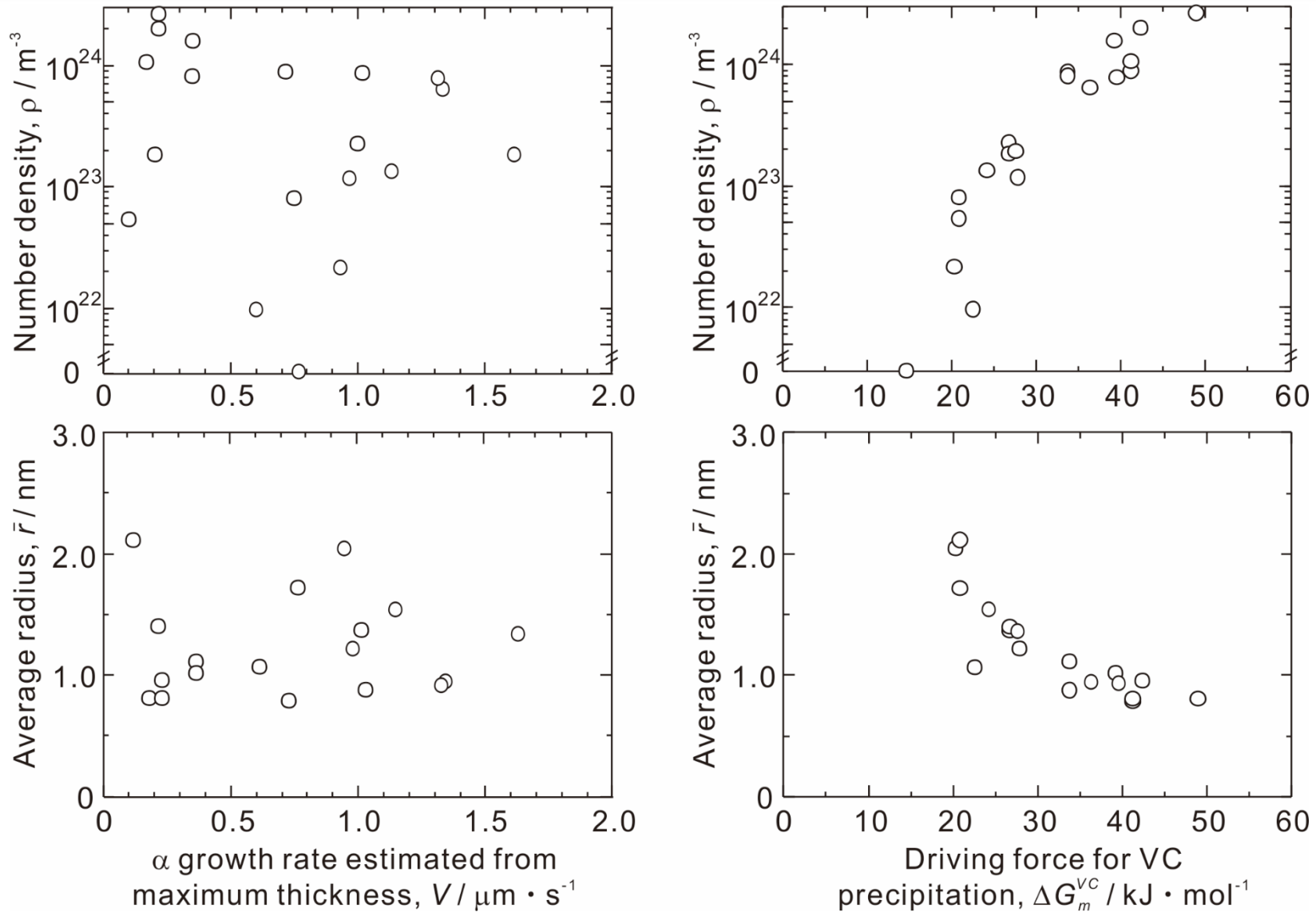


- α growth rate shows a peak at an intermediate temperature, becomes higher with lower Mn or higher Si content, and lower with higher C content.

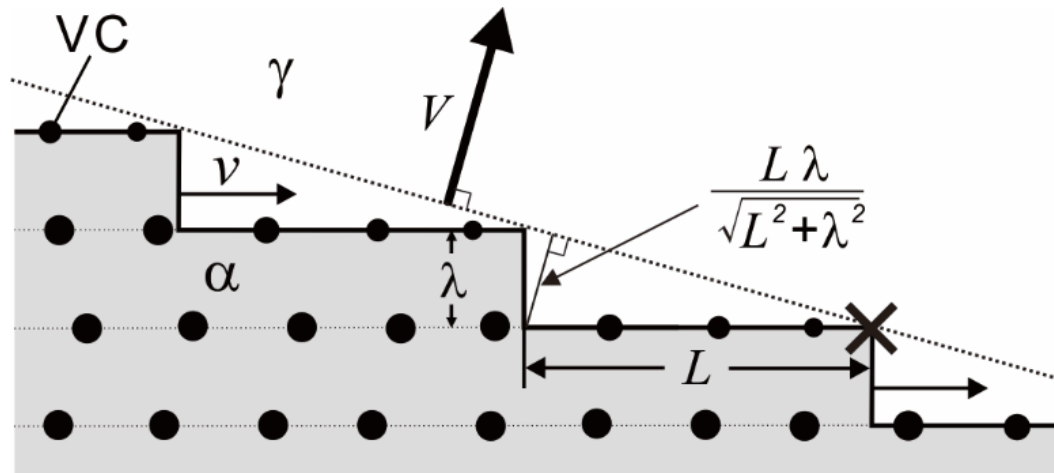
From interfacial composition:



- Driving force for precipitation is larger at lower temperature or with higher V, lower Mn or higher Si content, but not influenced by bulk C content.



- Compared with α growth rate, dispersion of VC shows better correlations with driving force for its precipitation.



V : macroscopic α growth rate;
 v : microscopic ledge growth rate;
 λ : ledge height;
 L : ledge distance

Aging time at migrating α/γ interface:

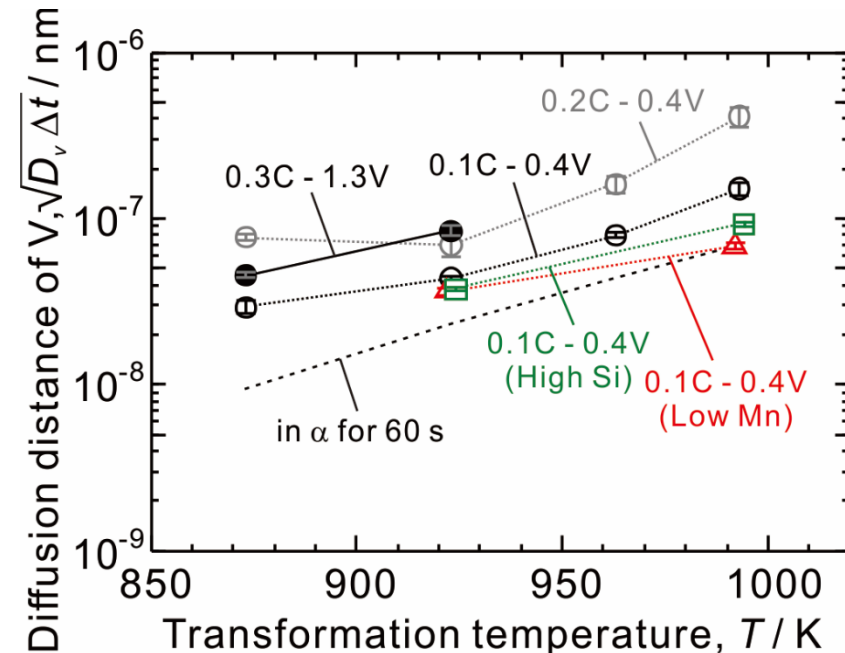
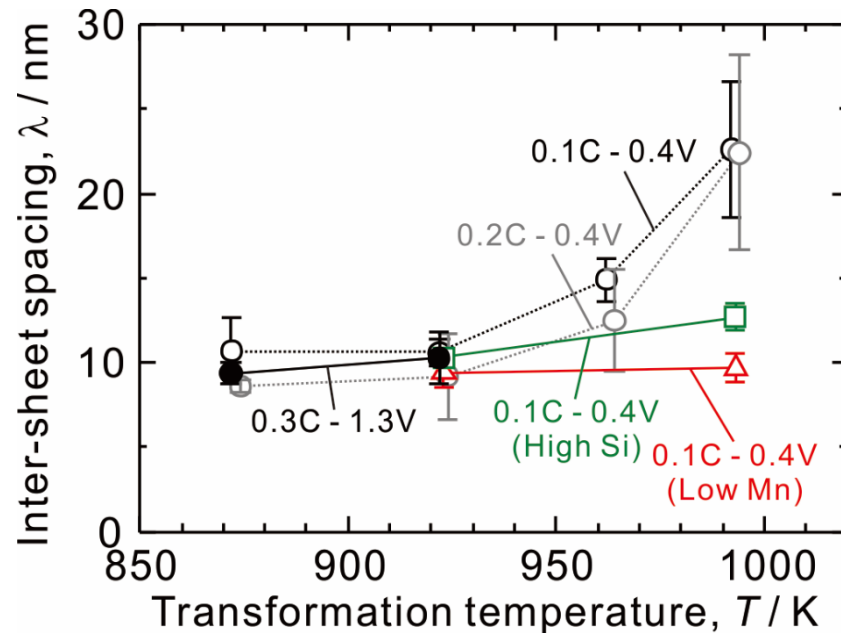
$$\Delta t = \frac{L}{v} = \frac{\frac{L\lambda}{\sqrt{L^2 + \lambda^2}}}{V} \approx \frac{\lambda}{V} \quad \text{when } L = 4\lambda$$

R. Okamoto al., *Acta Mater.*, 58 (2010) 4791.

- Aging time at migrating α/γ interface for precipitation of VC can be estimated from inter-sheet spacing and macroscopic α growth rate.

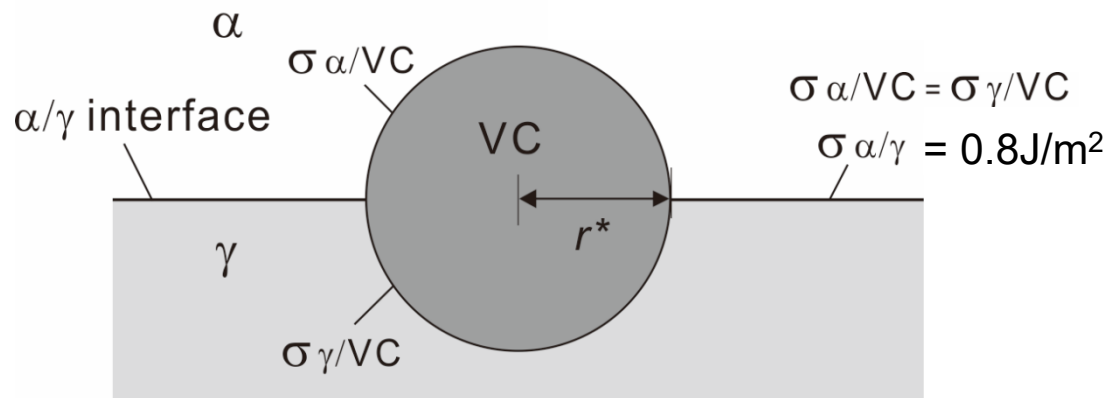
By using grain boundary diffusivity in Fe:

J. Fridberg et al., *Jernkontorets Ann.*, 153 (1969) 263.



- Inter-sheet spacing becomes smaller by lowering temperature, reducing Mn or increasing Si content at higher temperature.
- Interfacial aging time tends to be shorter with larger α growth rate.
- Interphase precipitation is mainly controlled by interfacial diffusion of V.

By assuming spherical critical nucleus:

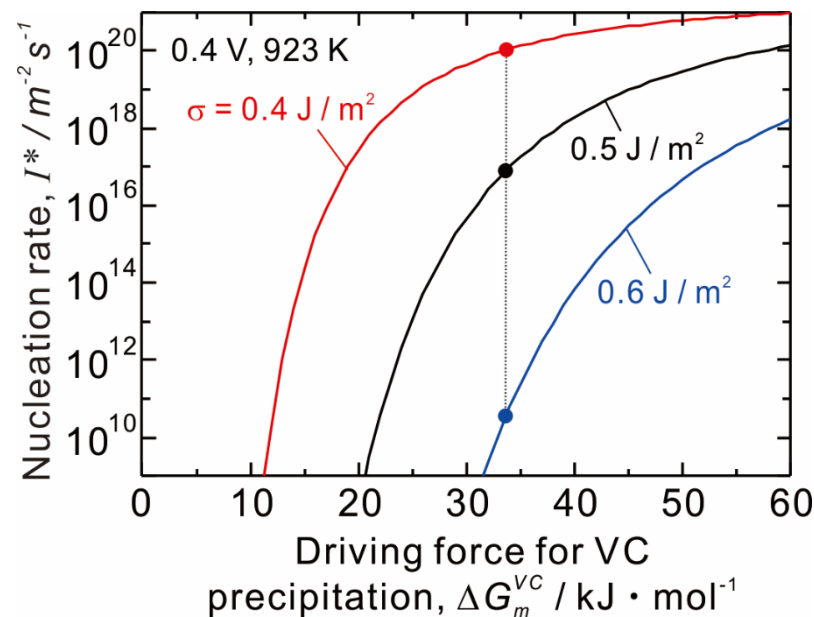
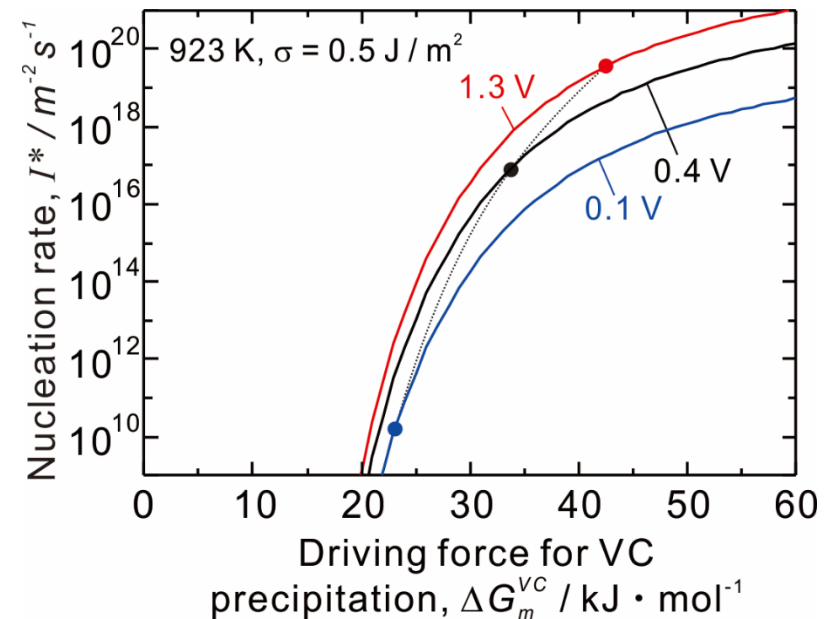
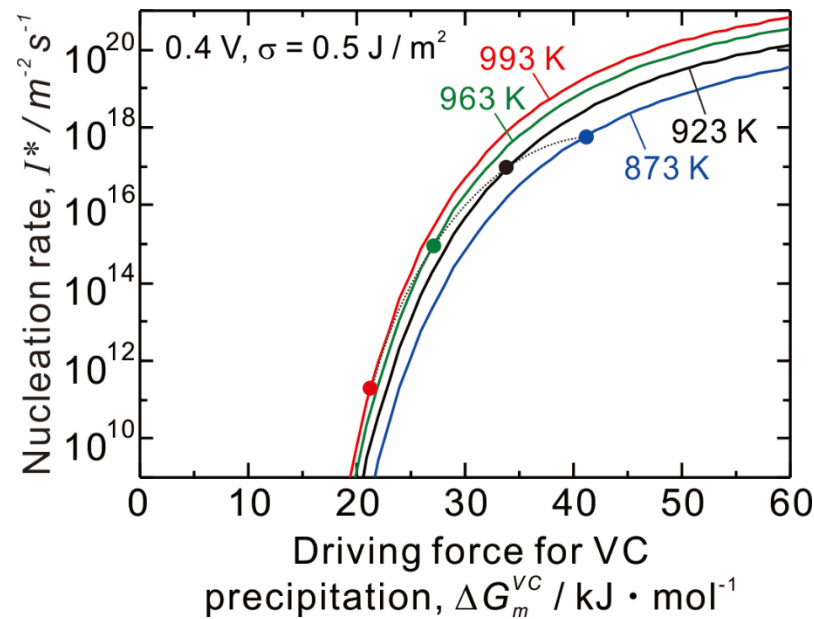


Nucleation rate:

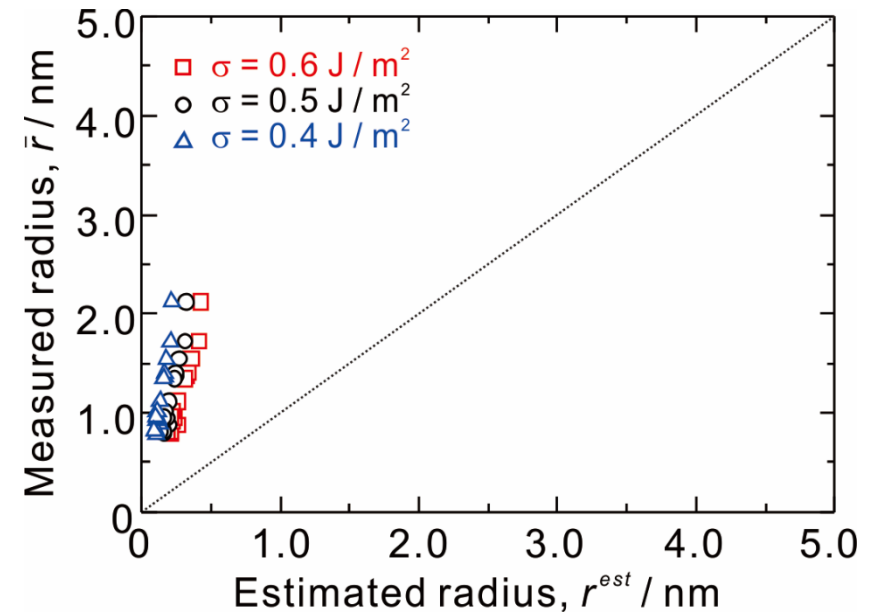
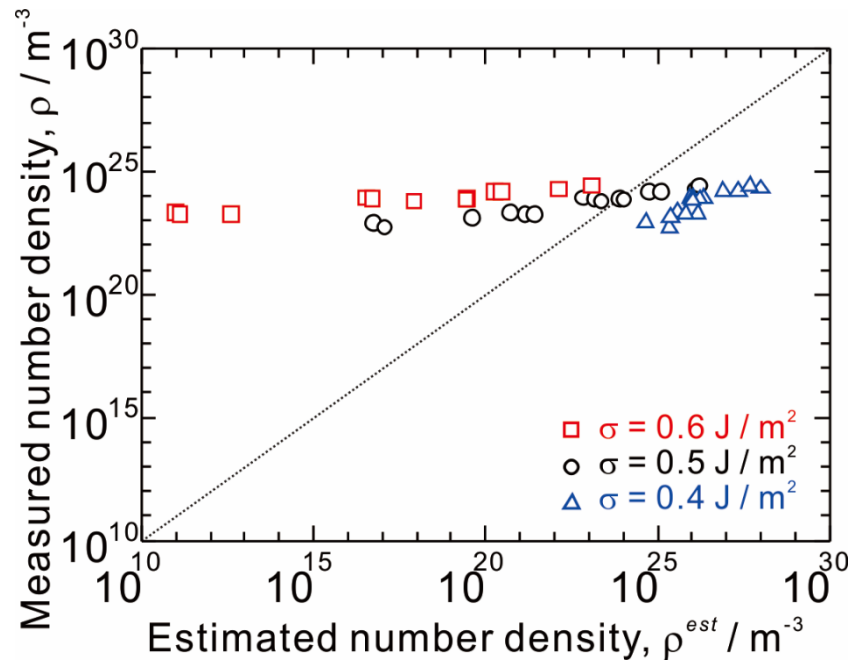
$$I^* = N\beta^*Z \exp\left(-\frac{\Delta G^*}{kT}\right)$$

N : density of nucleation site;
 β^* : frequency factor;
 Z : Zeldovich factor;
 ΔG^* : activation energy

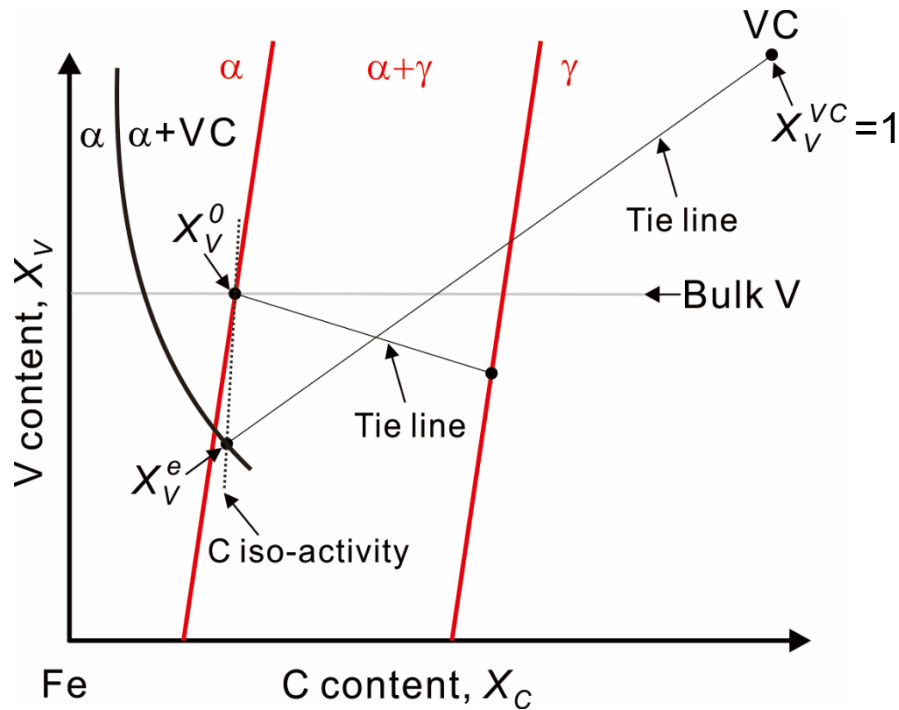
- N becomes larger with higher **bulk V content**.
- β^* becomes larger mainly by increasing **temperature**.
- Z becomes larger with larger **driving force for precipitation**, or with smaller **α/VC and γ/VC interfacial energy**.
- ΔG^* becomes smaller with larger **driving force for precipitation**, or with smaller **α/VC and γ/VC interfacial energy**.



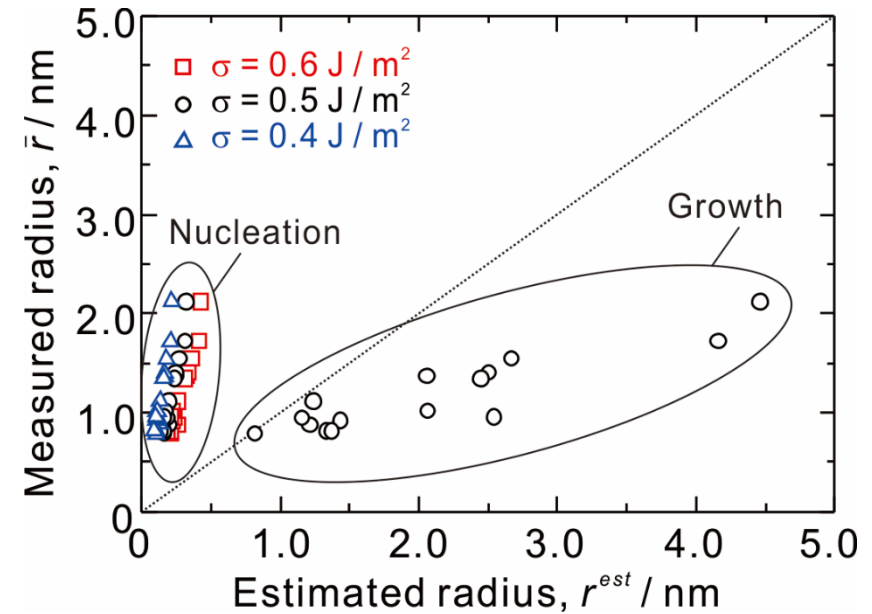
- Nucleation rate is significantly increased by lowering temperature, increasing V content, or lowering interfacial energy.



- Larger interfacial energy cannot reproduce variation range of number density, while small interfacial energy overestimate absolute amount.
- Regardless of interfacial energy, estimated radius is significantly smaller than measured ones.



By using interfacial diffusivity and aging time:



Radius after growth:

$$r = \sqrt{2 \frac{X_V^0 - X_V^e}{X_V^{VC} - X_V^e} D_V t}$$

X_V : V content;

D_V : interfacial diffusivity of V

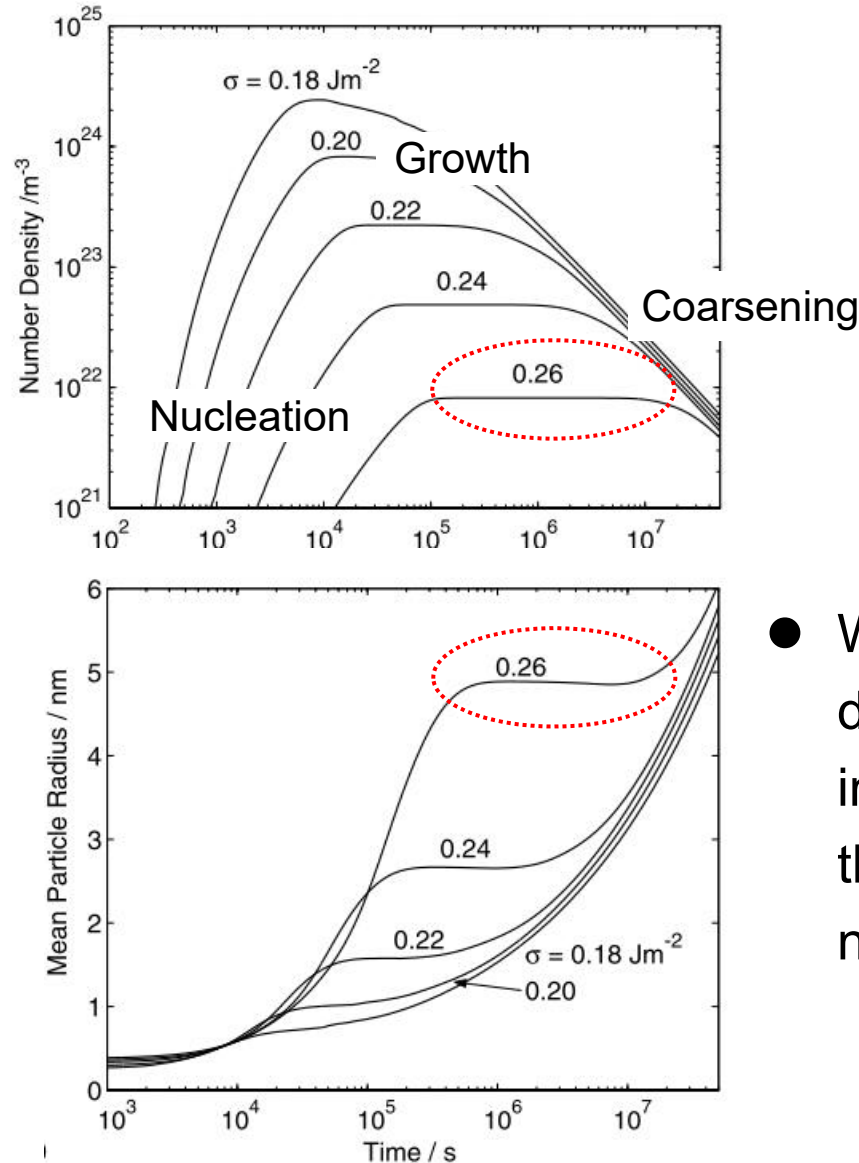
- Measured radius falls between those predicted ones for nucleation and growth.



Possible growth at migrating α/γ interface

Simulation of precipitation by aging (N model):

J.D. Robson, *Acta Mater.*, 52 (2004) 4669.



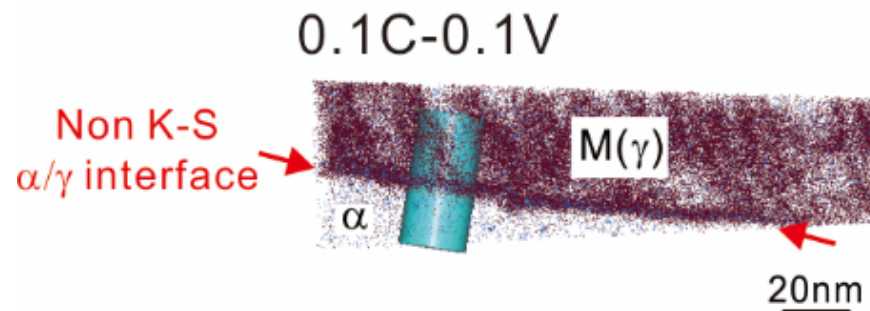
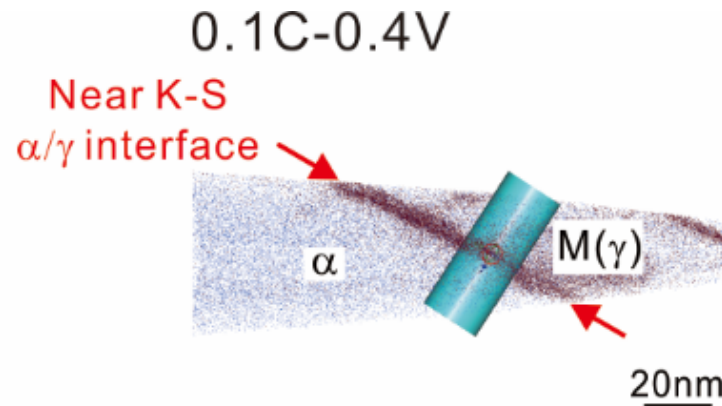
- Weak influence of α growth rate on dispersion of VC observed in this study implies that interphase precipitation is at the growth stage with plateau in both number density and size.

The effects of α growth rate and driving force for precipitation on dispersion of VC interphase precipitation were investigated.

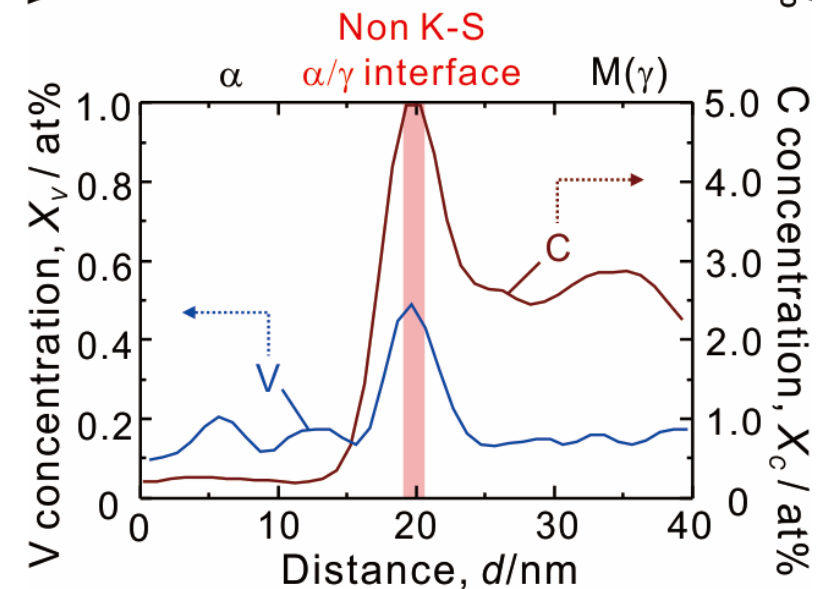
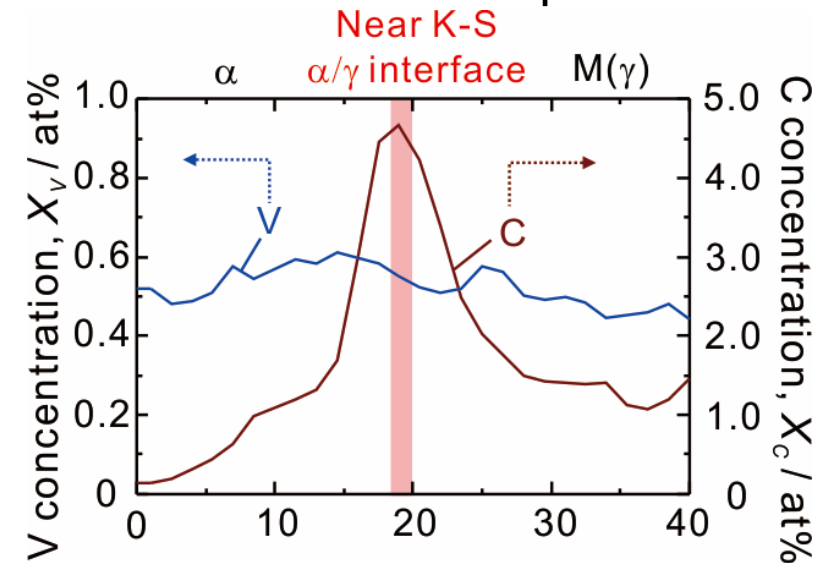
This study can be summarized as:

- Finer dispersion of VC formed by interphase precipitation can mainly be explained by larger driving force, while α growth rate only plays a minor role in influencing the dispersion.
This can be understood by considering both nucleation and growth kinetics of VC at migrating α/γ interface.

V + C atom map

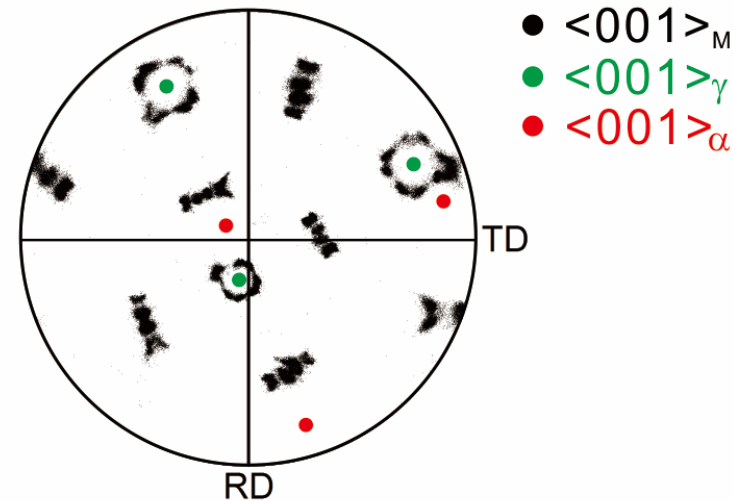
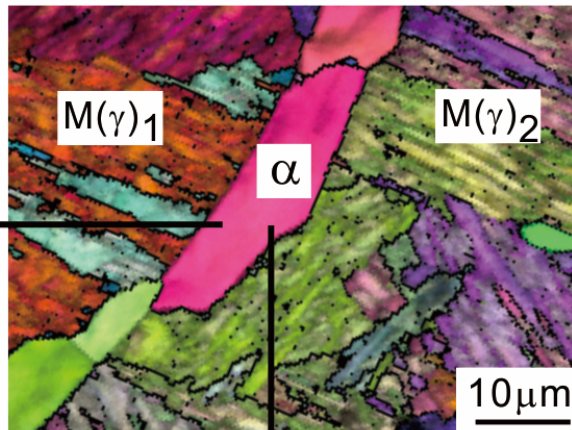


1D concentration profile



- In addition to C, V is also severely segregated at non K-S α/γ interface.

① EBSD \rightarrow α -orientation map + 001_{bcc} pole figure \rightarrow α/γ OR analyses:



Deviation angle from the exact K-S OR: $\Delta\theta$

Near K-S: $\Delta\theta \leq 5\text{deg.}$

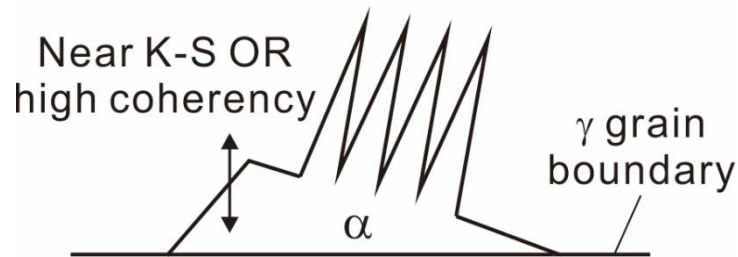
Non K-S: $\Delta\theta > 5\text{deg.}$

Micro-sampling by
focused ion beam

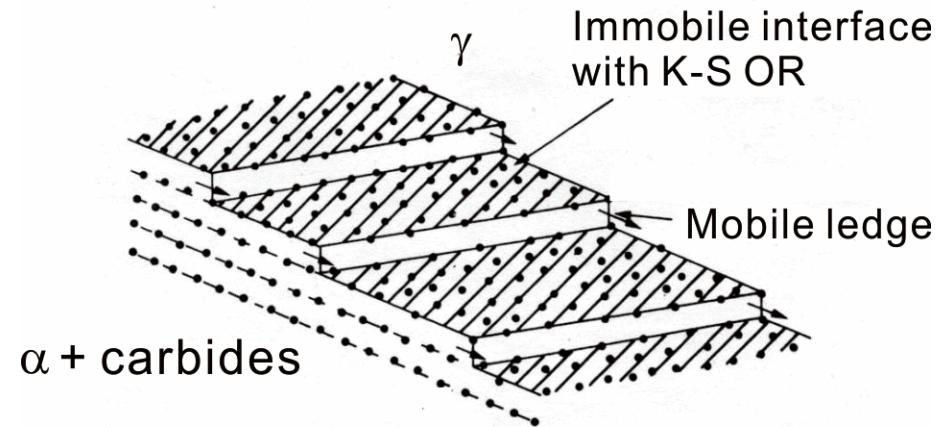
② 3DAP analyses \rightarrow dispersion of VC precipitates

③ Nano-indentation \rightarrow nanohardness of the same α grain

Ledge Mechanism

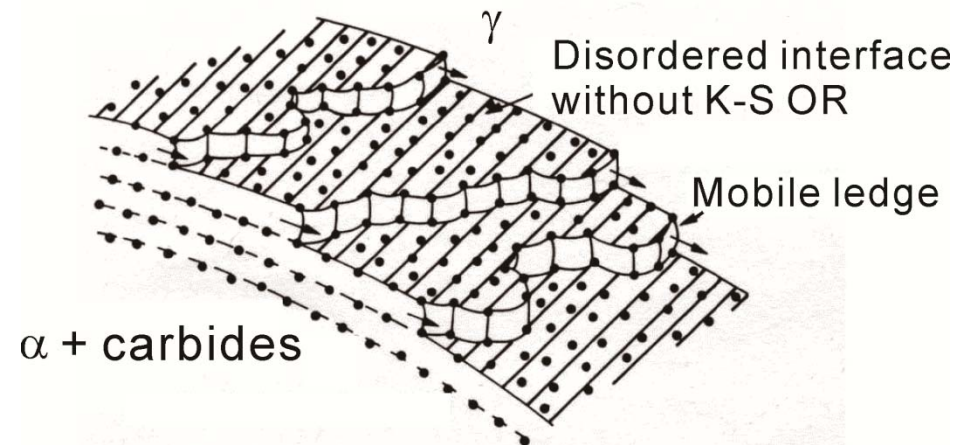
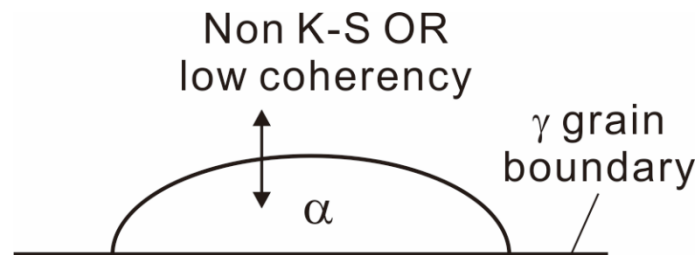


Kurdjumov-Sachs (K-S)
orientation relationship (OR):
 $(111)_{\gamma} // (011)_{\alpha}$, $[\bar{1}01]_{\gamma} // [\bar{1}\bar{1}1]_{\alpha}$



R.W.K. Honeycombe, *Metall. Mater. Trans. A* 7 (1976) 915.

Quasi-ledge Mechanism



R.A. Ricks et al., *Acta Metall.* 31 (1983) 853.

Ashby-Orowan model:

$$\Delta\tau = 0.84 \left(\frac{1.2Gb}{2\pi L} \right) \cdot \ln \frac{x}{2b}$$

$$x = 2\bar{r} \sqrt{\frac{2}{3}}$$

G : shear modulus of α ;

b : Burgers vector of α ;

L : inter-particle spacing of MC on slip plane;

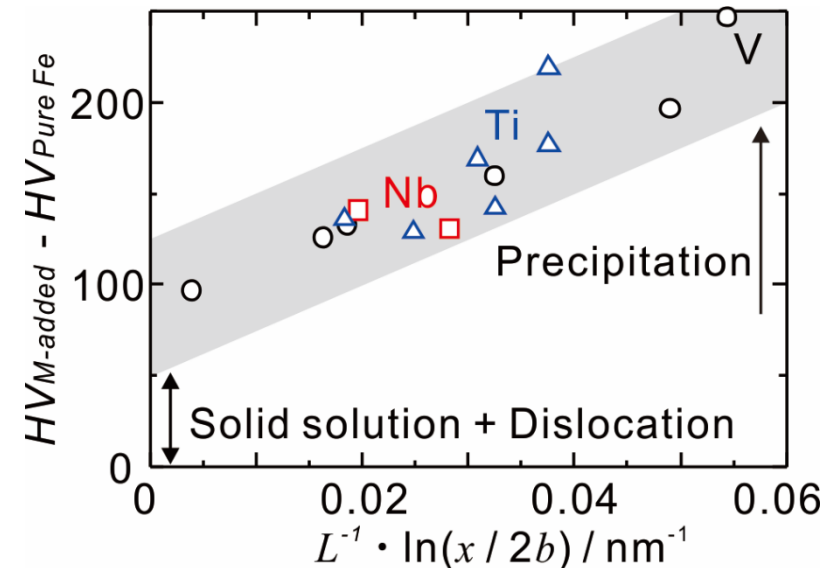
x : average diameter of MC on slip plane;

\bar{r} : average radius of MC

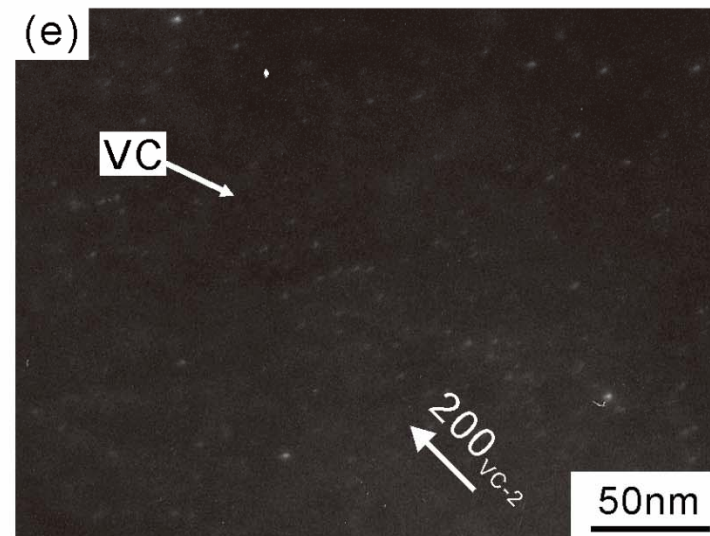
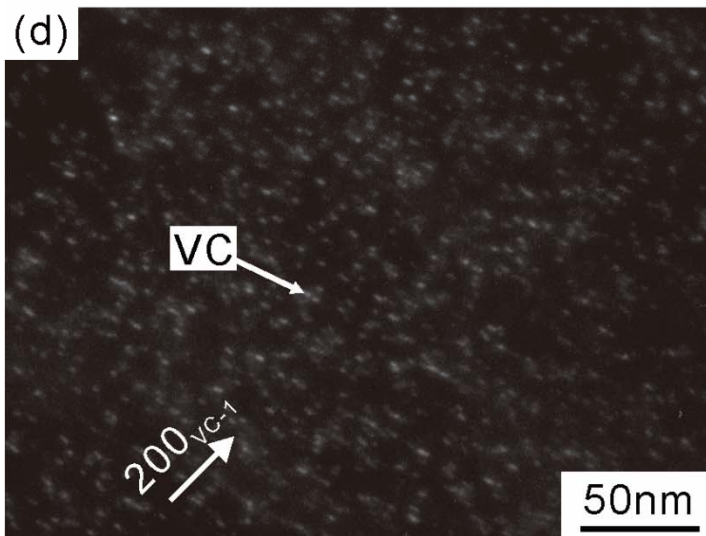
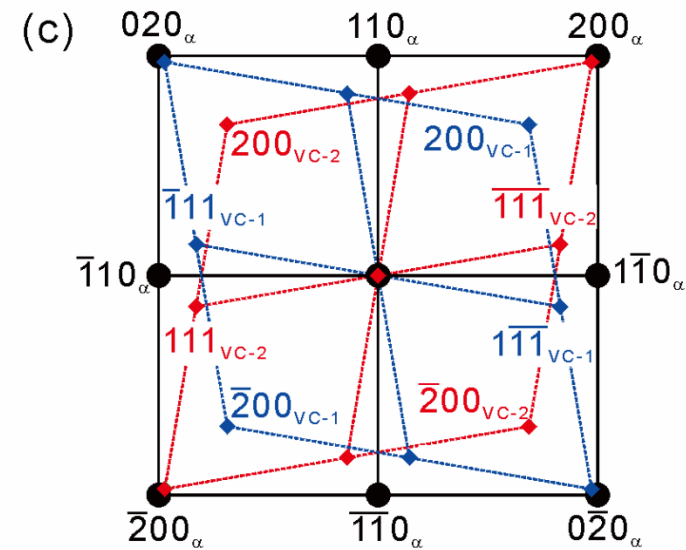
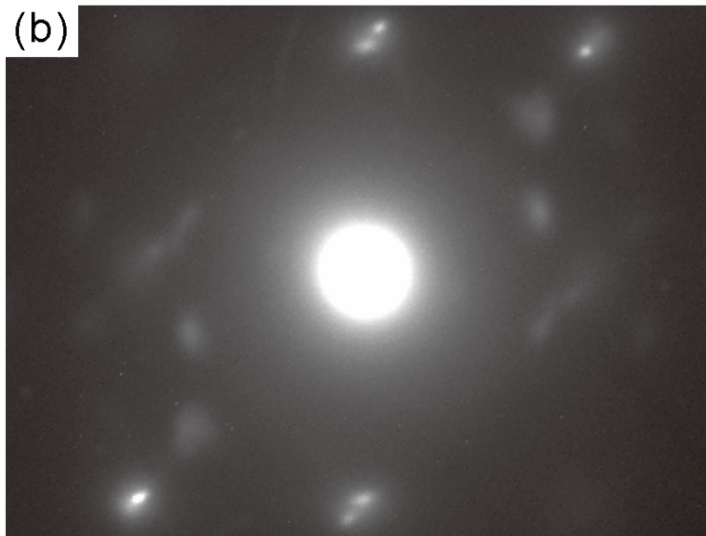
T. Gladman, *Mater. Sci. Tech.* 15 (1999) 30.

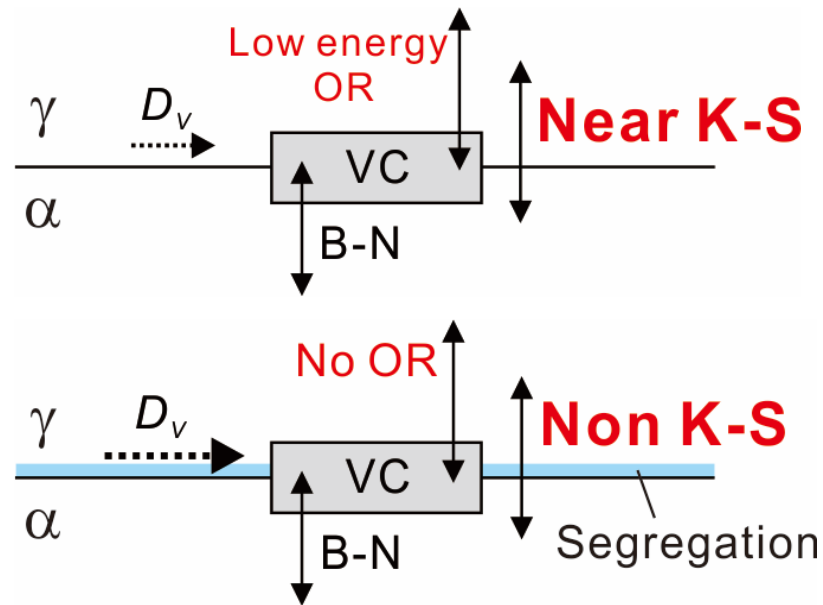
Hardness increment:

$$\begin{aligned} \Delta HV &= HV_{M-added} - HV_{Pure Fe} \\ &= HV_{ss} + HV_{disl} + HV_{ppt} \end{aligned}$$



- Higher hardness increment of α by precipitation strengthening can be obtained by reducing the inter-particle spacing of MC.





Baker-Nutting (B-N) OR:
 $(001)_{\alpha} // (001)_{VC}, [110]_{\alpha} // [100]_{VC}$

	σ (J / m ²)	Exp. / Calc.	Ref.
α/γ K-S	~0.3	Calc.	[1]
α/γ random	~0.8	Exp.	[2]
γ/VC semi-coh.	~1.9	Calc.	[3]
γ/VC incoh.	~2.6	Calc.	[3]
α/VC semi-coh.	~0.6	Calc.	[4]

$$\Delta\sigma \approx \sigma_{\alpha/VC} + \sigma_{\gamma/VC} - \sigma_{\alpha/\gamma}$$

$$= 2.2 \text{ J/m}^2 \quad \text{Near K-S case}$$

$$= 2.4 \text{ J/m}^2 \quad \text{Non K-S case}$$

- Promotion VC nucleation at non K-S interface is mainly caused by higher interfacial diffusivity and segregation of V, instead of higher α/γ interfacial energy.

[1] M. Enomoto et al., *PTM* (2005) 67.

[2] L.E. Murr, *Int. Phen. in Metals and Alloys* (1975) 124.

[3] T. Furuhashi et al., *ISIJ Int.* 43 (2003) 1630.

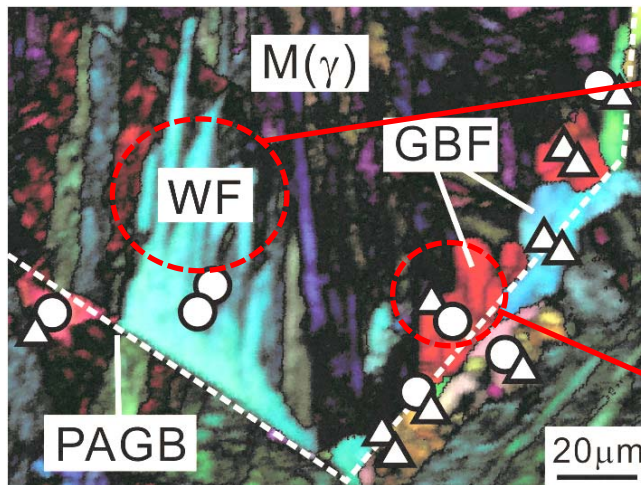
[4] D.H.R. Fors et al., *Phys. Rev. B.* 82 (2010) 195410.

923K, 60s

α orientation map

○ : Near K-S ($\Delta\theta \leq 5\text{deg.}$);

△ : Non K-S ($\Delta\theta > 5\text{deg.}$)



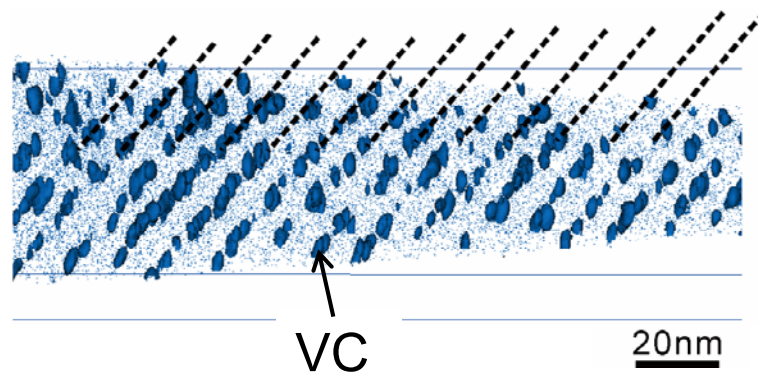
PAGB: prior γ grain boundary; M(γ): martensite;
GBF: grain boundary α ; WF: Widmanstätten α ;
 $\Delta\theta$: deviation angle from the exact Kurdjumov-Sachs orientation relationship (K-S OR)

Three-dimensional V atom map

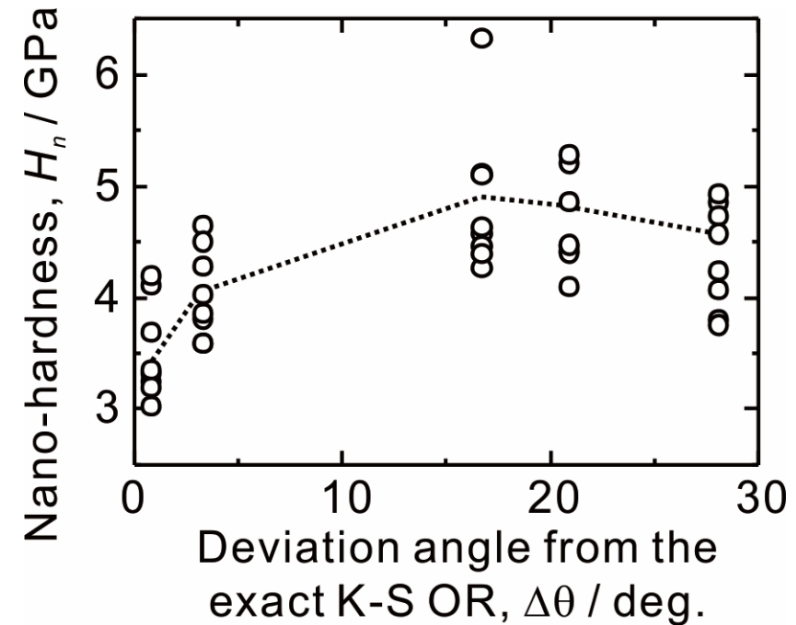
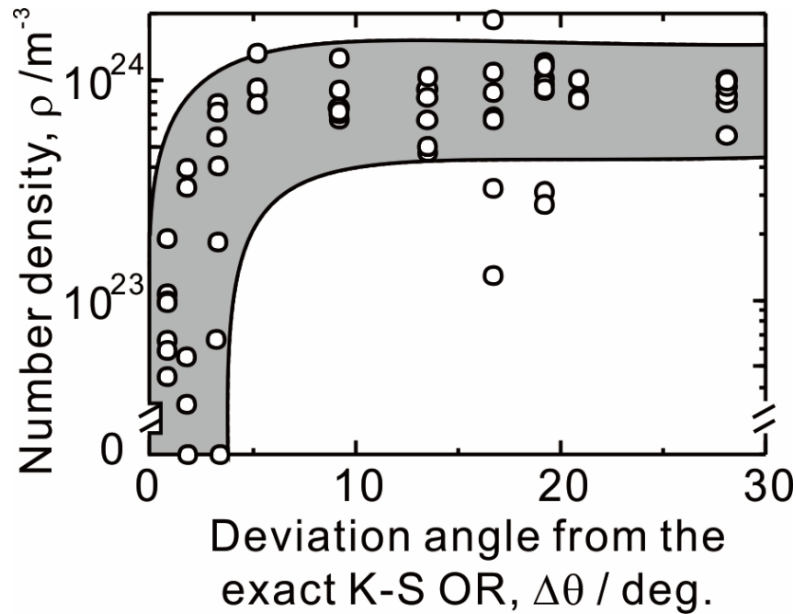
WF ($\Delta\theta = 0.8\text{deg.}$)



GBF ($\Delta\theta = 19.2\text{deg.}$)



- α transformation is proceeded by the migration of both near K-S and non K-S α/γ interface.
- Almost no VC precipitate exists in WF with near K-S OR, while VC interphase precipitation is observed in GBF with non K-S OR.



Y.-J. Zhang et al., *Scr. Mater.* 69 (2013) 17.

- As α/γ OR deviates from exact K-S, number density of VC increases significantly at first and remains almost constant later, while the size of VC is only slightly increased.
- Higher number density of VC in α grains with non K-S OR results in higher nanohardness compared with those with near K-S OR.